



Short communication

# Dynamics of four coupled phase-only oscillators

Richard Rand <sup>\*</sup>, Jeffrey Wong

*Department of Theoretical and Applied Mechanics, Cornell University, 207 Kimball Hall, Ithaca, NY 14853, United States*

Received 27 June 2006; accepted 27 June 2006

Available online 28 August 2006

---

## Abstract

We study the dynamics of a system of four coupled phase-only oscillators. This system is analyzed using phase difference variables in a phase space that has the topology of a three-dimensional torus. The system is shown to exhibit numerous phase-locked motions. The qualitative dynamics are shown to depend upon a parameter representing coupling strength. This work has application to MEMS artificial intelligence decision-making devices.

© 2006 Elsevier B.V. All rights reserved.

*PACS:* 02.30.Hq; 07.05.Mh; 07.10.Cm

*Keywords:* MEMS oscillators; Nonisolated equilibria; Phase-locked motion

---

## 1. Introduction

This work is motivated by recent developments in MEMS (Micro Electrical Mechanical Systems) involving the design and analysis of extremely small limit cycle oscillators [1,3](#). It has become feasible to build systems consisting of large numbers of coupled limit cycle MEMS oscillators. Analytical studies of coupled limit cycle oscillators have shown that such systems can exhibit diverse steady states, including, for example, spiral waves [4,7](#). In the case that there exist multiple stable periodic steady states, each steady state will have its own basin of attraction, i.e., those initial conditions which approach it. We may therefore envision an application in which such a system is used as a decision-making device: An initial condition is presented to the device and an output signal is generated which depends on which steady state is approached. For example imagine a radar system which alerts the operator that targets have been observed coming in from such and such a direction, and so on. Such systems have been identified as being analogous to brain models involving associative memory [2](#).

The purpose of this paper is to analyze the simplest such system of coupled oscillators. We have found that a system consisting of as few as four limit cycle oscillators exhibits qualitatively similar behavior to that of much larger systems. In particular, this includes the possibility of a continuum of stable nonisolated steady states.

---

<sup>\*</sup> Corresponding author. Fax: +1 607 255 2011.  
*E-mail address:* [rrh2@cornell.edu](mailto:rrh2@cornell.edu) (R. Rand).

For mathematical simplicity, we have chosen to model the individual oscillators as phase-only oscillators. These are related to more traditional models of limit cycle oscillators, such as van der Pol oscillators, via an approximate analysis involving a two-step process: (i) using averaging to replace the original equations by a *slow flow*, and (ii) truncating the slow flow by ignoring the amplitudes of vibration. This strategy goes back at least to 1980, where it was used in a study of two coupled van der Pol oscillators 6. In the case of a system of  $n$  coupled limit cycle oscillators of the form

$$\ddot{z}_i + z_i = \epsilon F_i(z_j, \dot{z}_j), \quad i, j = 1, \dots, n \tag{1}$$

one looks for a small- $\epsilon$  perturbation solution in the form  $z_i = R_i(t)\cos(t + \theta_i(t))$ . Using averaging or multiple scales 5, this gives a slow flow on  $R_i(t)$  and  $\theta_i(t)$ :

$$\dot{R}_i(t) = \epsilon G_i(R_j, \theta_j), \quad \dot{\theta}_i(t) = \epsilon H_i(R_j, \theta_j) \tag{2}$$

If in the uncoupled state, the  $i$ th oscillator exhibits a limit cycle with amplitude  $R_i = A_i$ , then we obtain an approximate slow flow by assuming that after coupling it continues to display a limit cycle with an amplitude that differs from  $A_i$  by  $O(\epsilon)$ . This gives the phase-only system:

$$\dot{\theta}_i(t) = \epsilon H_i(A_j, \theta_j) + O(\epsilon^2) \tag{3}$$

In the present paper we model a system of four phase-only oscillators by the following ODE's:

$$\dot{\theta}_1 = \omega + \sin(\theta_2 - \theta_1) + \sin(\theta_4 - \theta_1) + \alpha \sin(\theta_3 - \theta_1) \tag{4}$$

$$\dot{\theta}_2 = \omega + \sin(\theta_1 - \theta_2) + \sin(\theta_3 - \theta_2) + \alpha \sin(\theta_4 - \theta_2) \tag{5}$$

$$\dot{\theta}_3 = \omega + \sin(\theta_4 - \theta_3) + \sin(\theta_2 - \theta_3) + \alpha \sin(\theta_1 - \theta_3) \tag{6}$$

$$\dot{\theta}_4 = \omega + \sin(\theta_3 - \theta_4) + \sin(\theta_1 - \theta_4) + \alpha \sin(\theta_2 - \theta_4) \tag{7}$$

This system corresponds to the diagram shown in Fig. 1. Each oscillator is identical to the others with uncoupled limit cycle frequency of  $\omega$ . Coupling is via the sine function, the argument being the difference between the phase of a given oscillator and its neighbor. The coupling coefficient is taken as unity (without loss of generality) between oscillators having relative positions which are horizontal or vertical in Fig. 1, and is taken as  $\alpha$  between oscillators which are placed diagonally relative to one another.

These equations may be further simplified by replacing the dependent variables  $\theta_1, \theta_2, \theta_3, \theta_4$  by the phase differences  $\psi_1 = \theta_1 - \theta_4, \psi_2 = \theta_2 - \theta_4, \psi_3 = \theta_3 - \theta_4$ , thereby reducing the number of governing equations from 4 to 3:

$$\dot{\psi}_1 = \alpha \sin(\psi_3 - \psi_1) + \sin(\psi_2 - \psi_1) - \alpha \sin \psi_2 - \sin \psi_3 - 2 \sin \psi_1 \tag{8}$$

$$\dot{\psi}_2 = \sin(\psi_3 - \psi_2) - \sin(\psi_2 - \psi_1) - \sin \psi_3 - 2\alpha \sin \psi_2 - \sin \psi_1 \tag{9}$$

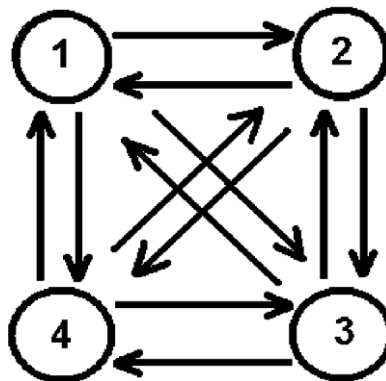


Fig. 1. A system of four coupled oscillators. The coupling coefficient is taken as unity between oscillators having relative positions which are horizontal or vertical, and is taken as  $\alpha$  between oscillators which are placed diagonally relative to one another. See Eqs. (4)–(7).

$$\dot{\psi}_3 = -\sin(\psi_3 - \psi_2) - \alpha \sin(\psi_3 - \psi_1) - 2 \sin \psi_3 - \alpha \sin \psi_2 - \sin \psi_1 \tag{10}$$

Note that an equilibrium point in Eqs. (8)–(10) represents a *phase-locked* periodic motion in physical coordinates  $z_i = R_i \cos(t + \theta_i)$ .

### 2. Analysis of the model

In this work we are interested in the qualitative nature of the solutions of Eqs. (8)–(10). To begin with we note that since the phase variables  $\psi_1, \psi_2$  and  $\psi_3$  are  $2\pi$ -periodic, the topology of the phase space is that of a three-dimensional torus,  $S \times S \times S$ . Thus we may represent the phase space by a cube with opposite sides identified, see Fig. 2. Note that all eight corners of the cube correspond to the same point. Note also that all arithmetic involving the  $\psi_i$  is mod  $2\pi$ .

The associated phase flow in the three-dimensional phase space of Fig. 2 possesses many symmetries. The flow (8)–(10) is said to be point-symmetric about the origin if replacing  $\psi_1, \psi_2, \psi_3$  by  $-\psi_1, -\psi_2, -\psi_3$  leaves the equations invariant. Point-symmetry about any other point  $(\psi_1^0, \psi_2^0, \psi_3^0)$  is defined by first moving the point to the origin by setting  $\psi_i = u_i + \psi_i^0$ , and then checking if the equations remain invariant when the  $u_i$  are replaced by  $-u_i$ . In this way we find that the flow (8)–(10) is point-symmetric about the following eight points:

$$\begin{aligned} A &= (0, 0, 0), & B &= (\pi, 0, \pi), & C &= (\pi, 0, 0), & D &= (0, 0, \pi), \\ E &= (\pi, \pi, \pi), & F &= (0, \pi, 0), & G &= (0, \pi, \pi), & H &= (\pi, \pi, 0). \end{aligned}$$

See Fig. 3 where these points are displayed. The point-symmetry plus the continuity of the vector field tells us that each of these points is an equilibrium for the flow (8)–(10). However, these points are not the only equilibria.

*Equilibria:* In addition to the equilibria A–H, there is a continuous ring of equilibrium points, each point of which is of the form:

$$I_k = (k, \pi, \pi + k) \tag{11}$$

where  $k$  is a parameter such that  $0 \leq k < 2\pi$ . Note that when  $k = 0$  the ring passes through the point  $G = I_0$  and when  $k = \pi$  it passes through  $H = I_\pi$ . See Fig. 4.

In the case that the coupling parameter  $|\alpha| > 1$ , there are four more equilibria given by the expressions:

$$J_1, J_2 = (\arccos(-1/\alpha), 0, -\arccos(-1/\alpha)) \tag{12}$$

$$L_1, L_2 = (\arccos(-1/\alpha), \arccos(2/\alpha^2 - 1), \arccos(-1/\alpha)) \tag{13}$$

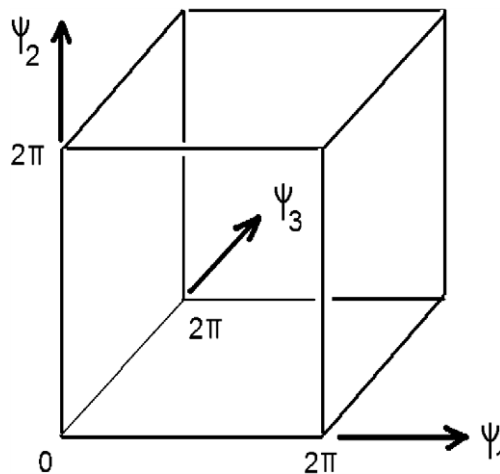


Fig. 2. The phase space of Eqs. (8)–(10) is a three-dimensional torus, represented here by a cube with opposite sides identified. Note that all eight corners of the cube correspond to the same point.

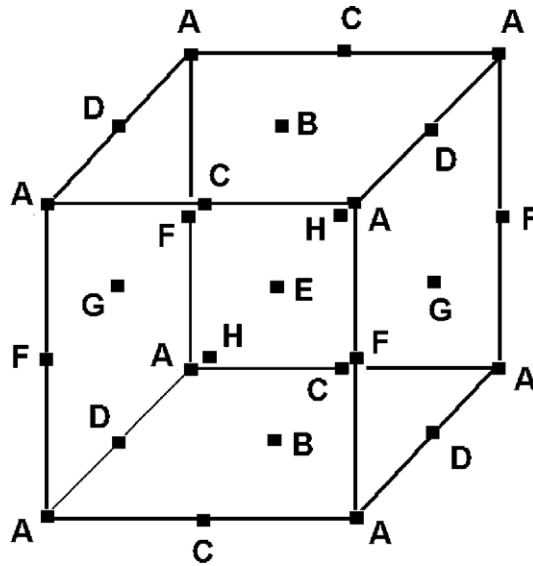


Fig. 3. Equilibrium points of the flow (8)–(10). All points shown lie on the surface of the cube except for point E which lies at the center of the cube. Points appear more than once because opposite sides of the cube are identified.

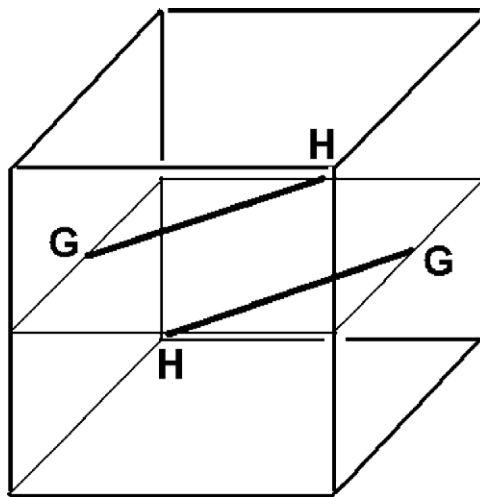


Fig. 4. A continuous ring of equilibrium points, each of which is of the form  $I_k = (k, \pi, \pi + k)$ , where  $0 \leq k < 2\pi$ . Points  $G = I_0$  and  $H = I_\pi$  of Fig. 3 lie in this ring.

The equilibria  $J_1, J_2, L_1, L_2$  are displayed in Fig. 5 for  $\alpha = -2$ . Note that  $J_1, J_2$  lie on the line

$$\psi_1 = -\psi_3, \quad \psi_2 = 0 \tag{14}$$

The line (14), shown dashed in Fig. 5, is an invariant line. (By definition, a set is invariant if any motion which starts in the set stays in it for all time). In fact, the line (14) is the intersection of two invariant planes. The flow (8)–(10) possesses the following five invariant planes:

$$\psi_2 = 0 \tag{15}$$

$$\psi_1 = \psi_3 \tag{16}$$

$$\psi_1 = \psi_2 + \psi_3 \tag{17}$$

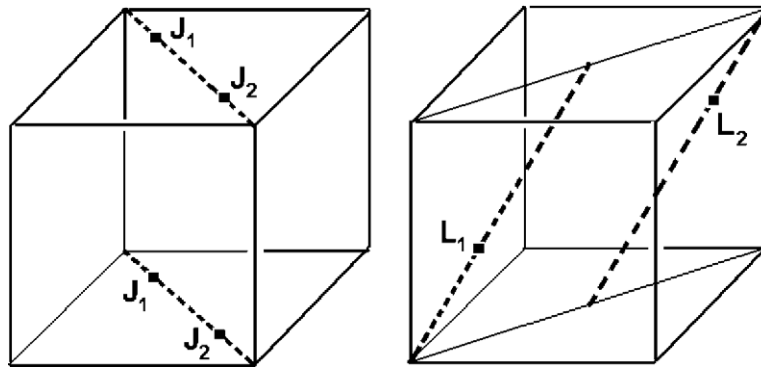


Fig. 5. Location of the equilibria  $J_1, J_2$  of Eq. (12) and  $L_1, L_2$  of Eq. (13) for  $\alpha = -2$ . These equilibria lie on the invariant lines (14) and (20) respectively. The invariant lines are shown dashed here in order to distinguish them from the ring of equilibria in Fig. 4.

$$\psi_2 = \psi_1 + \psi_3 \tag{18}$$

$$\psi_3 = \psi_1 + \psi_2 \tag{19}$$

(To show that each of these is an invariant plane, we show that they satisfy the differential equations (8)–(10) identically, that is, we differentiate each of them, then substitute in the flow (8)–(10) and finally use the original invariant equation to obtain an identity). Line (14) is the intersection of invariant planes (15) and (18). Similarly, equilibria  $L_1, L_2$  lie on the invariant line

$$\psi_1 = \psi_3, \quad \psi_2 = 2\psi_1 \tag{20}$$

which is the intersection of the two invariant planes (16) and (18).

*Stability:* The stability of the foregoing equilibria can be determined by computing the eigenvalues of the associated Jacobian matrix. This results in the following conclusions:

Point A is a sink for  $\alpha > -1$  and a saddle for  $\alpha < -1$ .

Point B is a source for  $\alpha < 1$  and a saddle for  $\alpha > 1$ .

Points C, D, E, F are saddles for all  $\alpha$ .

Points  $J_1, J_2$  and  $L_1, L_2$  are saddles when they exist, i.e. for  $|\alpha| > 1$ .

Points  $I_k$  (including points G and H) have eigenvalues  $2(\alpha - \cos k)$ ,  $2(\alpha + \cos k)$ , and 0. The 0 eigenvalue reflects the fact that these equilibria are part of a ring and are not isolated. Thus all points on the ring are sinks for  $\alpha < -1$ , and are sources for  $\alpha > 1$ . For values of  $\alpha$  between  $-1$  and  $1$ , the ring of nonisolated equilibria is composed of intervals which contain stable equilibria and other intervals which contain unstable equilibria.

### 3. Examples

#### Example 1. $\alpha = -2$

In this case point B is a source, the ring points  $I_k$  are all sinks, and all the other equilibria are saddles. Thus any initial condition will approach one of the ring points. If the ring were divided into  $n$  equal segments, then this scheme could be used to decompose the initial condition space into  $n$  basins of attraction. These could then be utilized in a decision-making application as discussed in the introduction.

#### Example 2. $\alpha = -1/2$

In this case point A is a sink, point B is a source and two intervals on the ring of equilibria are stable. All the other equilibria are saddles. The stable ring interval can be characterized by requiring the non-zero eigenvalues  $2(\alpha - \cos k)$  and  $2(\alpha + \cos k)$  to be negative. This gives that  $|\cos k| < 1/2$ . Thus a given initial condition could approach either point A or one of the ring points.

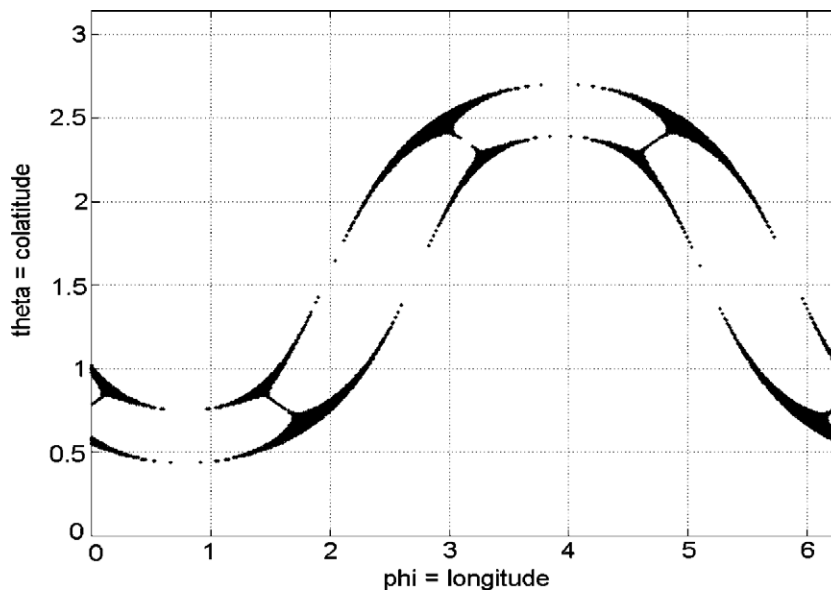


Fig. 6. Basins of attraction for  $\alpha = -1/2$ . Initial conditions are released from a sphere  $S$  of radius 0.1 centered at the source point B. Black points are initial conditions which do not approach the sink point A, but rather approach points on the ring of equilibria. The axes on this graph are polar coordinates  $\phi$  and  $\theta$ , where  $\psi_1 = \pi + 0.1\sin\theta\cos\phi$ ,  $\psi_2 = 0.1\cos\theta$  and  $\psi_3 = \pi + 0.1\sin\theta\sin\phi$ .

Since point B is the sole source, every point P in the phase space (except for a set of measure zero which lie on the stable manifolds of the saddles) has a corresponding point  $P_1$  which lies on a small sphere centered at B, such that  $P_1$  evolves to P for some time  $t$ . Equivalently, if the system is run backwards (by taking  $t$  into  $-t$ ), all points in the phase space (except for a set of measure zero) will approach B as  $t \rightarrow \infty$ . In order to determine the basins of attraction of the various stable steady states, we imagine a small sphere  $S$  centered at point B. Each point of  $S$ , if thought of as an initial condition, will approach either point A or a point on the ring of equilibria, or in the case of a set of measure zero, one of the saddles. See Fig. 6, where basins of attraction on the sphere  $S$  are displayed by using spherical polar coordinates.

#### 4. Structural stability

An objection to the practical application of the foregoing analysis to decision-making devices lies in the fact that it is well-known that a ring of equilibria is structurally unstable. Indeed we have found, for example, in the case of Example 1 above, for which the ring of equilibria are the only stable states, that if the uncoupled frequencies of the oscillators are not identical (that is,  $\omega$  in Eqs. (4)–(7)), then the ring of equilibria becomes replaced by a limit cycle. However, if the oscillator frequencies are very close to one another, then the time scale for the approach to the limit cycle is much faster than the period of the resulting limit cycle oscillation. Thus if one were to wait an appropriate length of time, an initial condition would get close to a point on the limit cycle which lies in the neighborhood of the point which would have been approached if the oscillators had truly identical frequencies. On a longer time scale the motion in question would move away from this point as it circulates around the limit cycle. Thus we believe that the method can be made practical by choosing the observation time appropriately.

#### 5. Conclusions

In conclusion we have shown that the simple system studied in this paper exhibits qualitatively similar behavior to that which has been observed in larger systems. For example, we have simulated the dynamics of a  $20 \times 20$  grid of identical phase-only oscillators, each coupled to four nearest neighbors (fewer for oscilla-

tors on the edge of the grid), and we have observed steady state dynamics which include, in addition to the in-phase mode, complicated stable spiral wave patterns which appear to be centered at an arbitrary point, i.e., evidently a continuum of stable steady states. The difficulty in understanding the geometry and topology of this 400 dimensional phase space led us to the work presented in this paper which is easier to visualize because it is three-dimensional, but yet which includes certain features which it shares with larger systems. The importance of such multiple and complicated steady states lies in possible applications to artificial intelligence decision-making devices.

### Acknowledgement

The authors wish to thank Anael Verdugo for his careful proofreading of this paper. This work was partially supported under the CMS NSF grant “Nonlinear Dynamics of Coupled MEMS Oscillators”.

### References

- [1] Aubin K, Zalalutdinov M, Alan T, Reichenbach RB, Rand R, Zehnder A, et al. Limit cycle oscillations in CW laser-driven NEMS. *J Microelectromech Syst* 2004;13:1018–26.
- [2] Hoppensteadt F, Izhikevich E. Oscillatory neurocomputers with dynamic connectivity. *Phys Rev Lett* 1999;82:2983–6.
- [3] Pandey M, Rand R, Zehnder A. Perturbation analysis of entrainment in a micromechanical limit cycle oscillator to appear. *Comm Nonlinear Sci Numer Simulat*, in press, [doi:10.1016/j.cnsns.2006.01.017](https://doi.org/10.1016/j.cnsns.2006.01.017).
- [4] Paullet JE, Ermentrout GB. Stable rotating waves in two-dimensional discrete active media. *SIAM J Appl Math* 1994;54:1720–44.
- [5] Rand RH. Lecture notes on nonlinear vibrations (version 52), available from: <http://www.tam.cornell.edu/randdocs> 2005.
- [6] Rand RH, Holmes PJ. Bifurcation of periodic motions in two weakly coupled van der Pol oscillators. *Int J Nonlinear Mech* 1980;15:387–99.
- [7] Strogatz SH. *Nonlinear dynamics and chaos*. Addison-Wesley; 1994.